Phase Geometry Series — Part I-B
Resonant Field Framework and Classical Basis for Magnetic Phase Control of a Thick SNS Weak Link

Aleksey Turchanov

November 2025

 Zenodo record DOI: 10.5281/zenodo.17807163

Abstract

We develop a two-layer description of magnetic phase control in superconducting weak links. On the effective level, we formulate a Resonant Field (RF) framework in which a weak link is treated as a *phase rotator*, characterized by a dimensionless phase–flux coefficient α and surrounded by a localized *Resonant Field Cell*. On the microscopic level, we show how the same objects and parameters arise from the standard theory of superconducting weak links: Ginzburg–Landau / Usadel equations for the order parameter, London–Maxwell electrodynamics for currents and fields, and the RCSJ model for Josephson phase dynamics. We identify the normalized phase response

$$\alpha = \frac{\Phi_0}{2\pi} \frac{\partial \varphi_J}{\partial \Phi_{\text{ext}}}, \tag{0.1}$$

and outline how thick SNS weak links with a local microcoil could reach the "strong rotator" regime $|\alpha| \sim 0.3$–0.6 under resonant conditions. Although we focus on thick SNS weak links with a local microcoil as a concrete experimental platform, the RF framework itself is not restricted to this particular geometry and can, in principle, be applied to any weak-link structure capable of supporting localized phase-field modes.

Within the broader Phase Geometry Series on superconductivity and weak gravity, this work plays the role of Part I-B: it supplies the calculational backbone that connects the conceptual Manifest I (Resonant Field Symmetry in Superconductors) to concrete device proposals on the superconducting side and to the phase-clock and gravity constructions developed in Parts II and III.

Contents

1 Introduction

Magnetic control of the Josephson phase is usually associated with macroscopic loops such as dc SQUIDs, where the total phase bias is proportional to the enclosed flux, $\varphi_J = (2\pi/\Phi_0)\Phi$. In contrast, a single weak link addressed by a local microcoil is typically assumed to be almost insensitive to magnetic flux: the phase only weakly responds to local fields because screening currents in the leads suppress the effective phase–flux coupling.

In Manifest I of the Phase Geometry Series, we introduced the idea that superconducting systems can host localized standing-field structures, *Resonant Field Cells*, which naturally act as *phase rotators*. A weak link that supports such a cell may then exhibit a much stronger local phase response than naïve estimates suggest.

The purpose of the present Part I-B is three-fold:

- to formulate an effective Resonant Field framework for magnetic phase control in weak links, introducing the notions of phase rotator, Resonant Field Cell, Phase–Control Equation and the key parameter α;
- to show how the same objects and parameters arise from the classical microscopic description (Ginzburg–Landau / Usadel + London–Maxwell + RCSJ);
- to provide an explicit dictionary between the RF language and the classical formalism.

We focus on thick SNS weak links driven by an on-chip microcoil and ask whether such structures can realistically reach a strong-rotator regime with $|\alpha| \sim 0.3$–0.6.

2 Part I: Resonant Field Framework

2.1 System geometry and experimental goal

We consider a superconducting strip interrupted by a central weak link of thickness d and lateral length L_W. A DC bias current I_{DC} flows along the strip, while an on-chip microcoil above the weak link carries an AC current $I_{AC}(t)$ and generates a local magnetic field $B_{AC}(t)$ through a thin insulating layer; see Fig. 1.

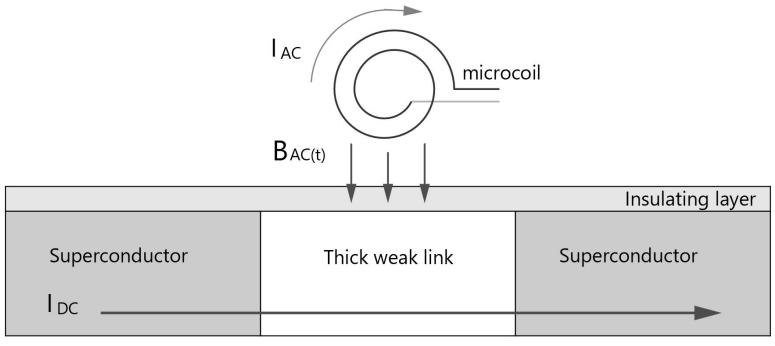

Figure 1: Geometry of a superconducting strip with a central thick weak link and an on-chip microcoil. A DC bias current I_{DC} flows along the strip, while an AC current I_{AC} in the microcoil generates a local magnetic field $B_{AC}(t)$ in the weak-link region through a thin insulating layer.

The experimental goal is to quantify how efficiently the local flux from the microcoil can rotate the Josephson phase across the weak link, and how this efficiency depends on the thickness d and on dynamical effects such as resonances.

2.2 Phase field and phase flow

In the RF language, the superconducting state is described by a phase field $\phi(\mathbf{r})$ defined over the strip, with supercurrent lines following the gradients of this field. When a weak link is present, the phase drop φ_J across it becomes a key degree of freedom.

The RF framework focuses on how phase flow is redistributed in response to local fields and how part of the energy may be stored in localized magnetic structures rather than purely in longitudinal phase gradients.

2.3 Phase rotator

A *phase rotator* is a localized element in which a relatively small change in external magnetic flux produces a significant change in the phase drop φ_J. Quantitatively, we introduce the phase–flux coefficient α via

$$\delta\varphi_J = \frac{2\pi}{\Phi_0}\,\alpha\,\delta\Phi_{\text{ext}}, \tag{2.1}$$

so that $\alpha = 1$ corresponds to the ideal SQUID limit.

Thin tunnel junctions typically realize $|\alpha| \ll 10^{-2}$ and are thus *weak rotators*. Thick SNS bridges, under appropriate conditions, may become *strong rotators* with $|\alpha| \sim 0.3$–0.6.

2.4 Resonant Field Cell

We define a *Resonant Field Cell* as a localized standing-field structure around the weak link in which phase, supercurrent and magnetic field form a self-consistent resonant pattern. Conceptually, the cell plays the role of a miniature cavity coupled to the weak link.

In thin junctions the RF Cell is absent or extremely rigid; in thick SNS bridges it can be well-localized around the weak link and store a non-trivial amount of magnetic tension. Figure 2 shows a qualitative sketch.

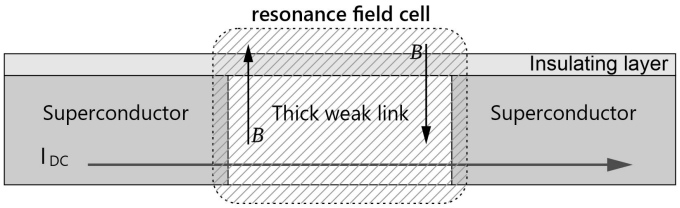

Figure 2: Qualitative picture of a Resonant Field Cell around a thick weak link. The shaded region marks the localized cell, and the opposite vertical arrows B schematically indicate a standing magnetic-field pattern inside the cell.

2.5 Phase–flux coefficient α

Within the RF framework we treat the total phase drop across the junction as

$$\varphi_J = \varphi_{\text{bias}} + \frac{2\pi}{\Phi_0}\,\alpha\,\Phi_{\text{ext}}, \tag{2.2}$$

where φ_{bias} is the phase set by the DC current bias, and Φ_{ext} is the flux created by the microcoil.

The dimensionless coefficient α encodes how strongly the RF Cell around the weak link couples the external flux to the Josephson phase. In the tunnel limit $|\alpha| \ll 10^{-2}$; in the strong-rotator regime we aim at $|\alpha| \sim 0.3$–0.6.

2.6 Phase–Control Equation

In the small-signal limit we can write the *Phase–Control Equation* as

$$\varphi_J(t) = \varphi_{\text{bias}}(t) + \frac{2\pi}{\Phi_0}\,\alpha\,\Phi_{AC}(t), \tag{2.3}$$

where $\Phi_{AC}(t)$ is the time-dependent coil flux. This effective equation captures the net result of microscopic screening currents and localized field patterns, and will later be derived from the RCSJ model in the classical formalism.

2.7 Static regimes: thin vs thick weak links

2.7.1 Thin barrier: negligible rotator

For an SIS tunnel junction with $d \ll \xi$, the phase jump is concentrated in a very narrow region, the local magnetic field is small, and the effective phase–flux coupling is strongly screened. In RF terms:

- the RF Cell is either absent or extremely rigid;
- $|\alpha(d)| \ll 10^{-2}$ for typical geometries;
- the weak link acts as a negligible rotator.

2.7.2 Thick SNS bridge: emergence of a strong rotator

When the thickness d of an SNS weak link is comparable to the coherence length ξ, the phase drop φ_J is distributed over a wider region, and a localized standing structure of currents and fields can appear around the bridge. In RF language:

- a well-defined RF Cell forms around the weak link;
- part of the energy is stored in local magnetic tension rather than purely longitudinal phase flow;
- the effective coupling $\alpha(d)$ can become significantly larger than in the tunnel limit.

Figure 3 illustrates the contrast between thin and thick regimes in terms of phase profiles and field patterns.

2.8 Dynamical regime and Shapiro steps

In the presence of a DC bias I_{DC} and an AC phase modulation, the Josephson relation

$$I(t) \approx I_c \sin\varphi_J(t) \tag{2.4}$$

leads to Shapiro steps on the I–V characteristic when the phase is locked to an external frequency ω.

Using the Phase–Control Equation with

$$\Phi_{AC}(t) = \Phi_0^{(\text{coil})} \sin\omega t, \tag{2.5}$$

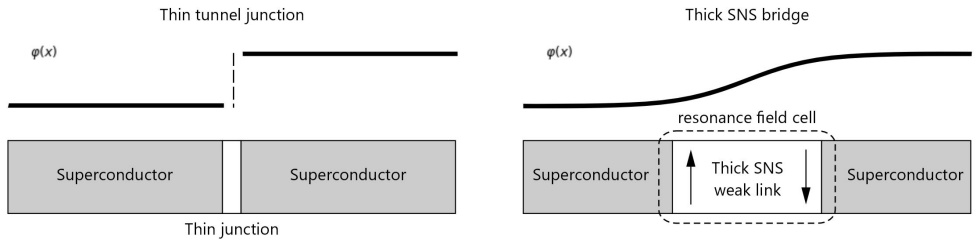

Figure 3: Qualitative comparison of phase profiles and field patterns for a thin tunnel junction (left) and a thick SNS bridge (right). In the tunnel limit the phase jump $\varphi(x)$ is sharply localized at the barrier and the local field structure is negligible; in the thick SNS regime the phase drop is distributed across the normal region and a localized RF Cell can form around the bridge.

we obtain a phase modulation amplitude

$$\Delta\varphi_{\mathrm{coil}} = \alpha \, \frac{2\pi}{\Phi_0} \, \Phi_0^{(\mathrm{coil})}. \tag{2.6}$$

The heights of Shapiro steps depend on $\Delta\varphi_{\mathrm{coil}}$, so by comparing coil-driven Shapiro steps with those produced by a calibrated RF voltage drive, one can experimentally infer α.

In the RF picture, a weak rotator ($|\alpha| \ll 10^{-2}$) will produce negligible Shapiro steps under coil-only drive, while a strong rotator ($|\alpha| \sim 0.3$–0.6) will show clear steps even without direct RF excitation of the junction.

2.9 Qualitative prediction for $\alpha(d)$ and target regime

The RF framework predicts a non-monotonic dependence of $|\alpha(d)|$ on the thickness d of the weak link:

- for $d \ll \xi$: tunnel regime, $|\alpha(d)| \ll 10^{-2}$;
- for $d \sim \xi$: thick SNS regime, formation of a strong RF Cell, and a qualitative transition from negligible magnetic response to a strong rotator;
- for $d \gg \xi$: degradation of superconducting coupling, smearing of the RF Cell, and a reduction of $|\alpha(d)|$.

We introduce a target range for the strong-rotator regime:

$$|\alpha_{\mathrm{target}}| \sim 0.3\text{–}0.6, \qquad d \sim \xi, \tag{2.7}$$

corresponding to a 2–3 orders-of-magnitude enhancement of the local phase sensitivity compared to the tunnel limit. Figure 4 shows a qualitative sketch.

The detailed shape of $\alpha(d)$ must ultimately be obtained from microscopic calculations (Part II) or from experiments (e.g. thick SNS bridges with microcoils). A simple order-of-magnitude estimate for realistic SNS bridges and microcoils is given in Appendix B.

3 Part II: Classical Description of the Same System

3.1 Geometry and parameters

We now turn to the standard classical description of the same system: a superconducting strip with a central weak link and a local microcoil, as in Fig. 1. The weak link may be:

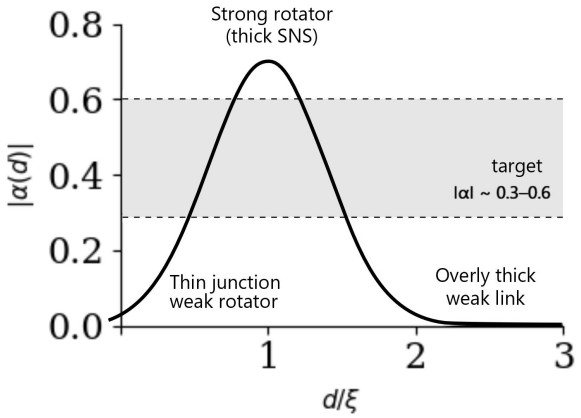

Figure 4: Qualitative sketch of $|\alpha(d)|$ versus normalized thickness d/ξ: small in the tunnel limit, peaking in the thick SNS regime, and decreasing for very large d. The shaded region indicates the target strong-rotator range $|\alpha| \sim 0.3$–0.6.

- an SIS tunnel junction with barrier thickness d;
- an SNS bridge where the normal layer has thickness d and length L_W;
- a nanobridge with an effective normal region.

Material parameters include the coherence length ξ, London penetration depth λ_L, normal resistance R_N of the weak link, and capacitance C.

3.2 Order parameter, phase, and supercurrent

The superconducting state is described by a complex order parameter

$$\Psi(\mathbf{r}) = |\Psi(\mathbf{r})| e^{i\theta(\mathbf{r})}, \tag{3.1}$$

with phase $\theta(\mathbf{r})$. In the GL/London approximation the supercurrent density is

$$\mathbf{j}_s(\mathbf{r}) = \frac{2e\hbar}{m^*} |\Psi(\mathbf{r})|^2 \left(\nabla\theta(\mathbf{r}) - \frac{2e}{\hbar} \mathbf{A}(\mathbf{r}) \right), \tag{3.2}$$

where $\mathbf{A}$ is the vector potential and $\mathbf{B} = \nabla \times \mathbf{A}$.

3.3 Weak link and Josephson phase

Let θ_L and θ_R be the phases in the left and right superconducting banks. The Josephson phase is

$$\varphi_J = \theta_R - \theta_L + \frac{2\pi}{\Phi_0} \Phi_{\text{int}}, \tag{3.3}$$

where Φ_{int} represents the internal flux contribution associated with the weak-link region. The current–phase relation is

$$I_s = I_c(d) \sin \varphi_J, \tag{3.4}$$

with $I_c(d)$ depending on the type and thickness of the weak link.

3.4 Static field distributions and thick SNS regime

In a thin tunnel junction:

- $\theta(\mathbf{r})$ changes abruptly across the barrier;
- $|\Psi|$ is reduced only in a narrow region;
- the local magnetic field associated with the junction is small.

In a thick SNS bridge ($d \sim \xi$):

- the phase $\theta(x)$ varies smoothly across the normal region;
- supercurrents and fields can form extended localized patterns around the bridge;
- the system may support normal modes localized near the weak link.

These localized modes are the classical counterpart of the RF Cells introduced earlier.

3.5 RCSJ model and external flux

The dynamics of the Josephson phase is described by the RCSJ model

$$C\ddot{\varphi}_J + \frac{1}{R}\dot{\varphi}_J + I_c \sin\varphi_J = I_{\text{bias}} + I_{\text{noise}}, \tag{3.5}$$

where C is the junction capacitance, R the shunt resistance, I_{bias} the bias current, and I_{noise} a noise term.

A current $I_{\text{coil}}(t)$ in the microcoil produces an external flux

$$\Phi_{\text{ext}}(t) = M I_{\text{coil}}(t), \tag{3.6}$$

where M is the mutual inductance between the coil and the effective phase-sensitive loop. Due to screening and geometry, only a fraction $\eta(d)$ of Φ_{ext} actually contributes to the phase:

$$\Phi_{\text{eff}}(t) = \eta(d)\,\Phi_{\text{ext}}(t). \tag{3.7}$$

The phase then acquires an additional term

$$\varphi_J(t) = \varphi_0(t) + \frac{2\pi}{\Phi_0}\,\Phi_{\text{eff}}(t), \tag{3.8}$$

where $\varphi_0(t)$ is the phase in the absence of external flux.

3.6 Classical definition of α and upper bound

Comparing with the general linear-response form

$$\delta\varphi_J(t) = \left.\frac{\partial\varphi_J}{\partial\Phi_{\text{ext}}}\right|_0 \delta\Phi_{\text{ext}}(t), \tag{3.9}$$

we identify

$$\frac{\partial\varphi_J}{\partial\Phi_{\text{ext}}} = \frac{2\pi}{\Phi_0}\,\eta(d), \tag{3.10}$$

and thus

$$\alpha(d) = \frac{\Phi_0}{2\pi}\frac{\partial\varphi_J}{\partial\Phi_{\text{ext}}} = \eta(d). \tag{3.11}$$

In an ideal SQUID loop with flux Φ we have $\varphi_J = (2\pi/\Phi_0)\Phi$, hence $\alpha_{\mathrm{SQUID}} = 1$. Any realistic local-coil geometry without a full loop must satisfy $|\eta(d)| < 1$, therefore

$$0 < |\alpha(d)| \leq 1. \tag{3.12}$$

The interval $0 < \alpha \leq 1$ used in the RF framework is thus naturally interpreted as a normalization with respect to the SQUID limit.

For typical thin tunnel junctions without special field focusing one expects $\eta \sim 10^{-3}$–10^{-2}, giving

$$|\alpha_{\mathrm{static}}| \sim 10^{-3}\text{–}10^{-2} \tag{3.13}$$

for the static response, in agreement with the intuition that a single junction is almost insensitive to a local coil in the absence of a loop.

3.7 Oscillator estimate for $\alpha(\omega)$

To capture dynamical effects, we linearize the RCSJ equation around a static operating point and include the coil drive:

$$C\ddot{\varphi} + \frac{1}{R}\dot{\varphi} + \frac{1}{L_J}\varphi = KI_{\mathrm{coil}}(t), \tag{3.14}$$

where L_J is the Josephson inductance (around the operating point) and K is a coupling coefficient. The plasma frequency and damping rate are

$$\omega_p = \sqrt{\frac{1}{L_J C}}, \qquad \gamma = \frac{1}{2RC}. \tag{3.15}$$

For a harmonic drive $I_{\mathrm{coil}}(t) = I_0 e^{i\omega t}$ the steady-state solution gives an effective phase response

$$\alpha_{\mathrm{eff}}(\omega) = \frac{\Phi_0}{2\pi}\frac{\partial\varphi_J(\omega)}{\partial\Phi_{\mathrm{ext}}(\omega)} \propto \frac{1}{\sqrt{(\omega_p^2 - \omega^2)^2 + (2\gamma\omega)^2}}. \tag{3.16}$$

In the quasistatic limit $\omega \ll \omega_p$ we have

$$\alpha_{\mathrm{static}} \equiv \alpha_{\mathrm{eff}}(0) \propto \frac{1}{\omega_p^2}, \tag{3.17}$$

while at resonance ($\omega = \omega_p$),

$$\alpha_{\mathrm{res}} \equiv \alpha_{\mathrm{eff}}(\omega_p) \propto \frac{1}{2\gamma\omega_p}. \tag{3.18}$$

Eliminating the prefactor yields

$$\alpha_{\mathrm{res}} \approx \alpha_{\mathrm{static}}\,\frac{\omega_p}{2\gamma} = \alpha_{\mathrm{static}} Q, \tag{3.19}$$

where $Q = \omega_p/(2\gamma)$ is the quality factor of the mode.

Figure 5 shows the corresponding qualitative frequency dependence. A standard oscillator derivation of this relation is summarized in Appendix A.

4 Part III: Mapping Between RF and Classical Frameworks

The preceding sections show that all objects of the RF framework have explicit counterparts in the classical description. Figure 6 summarizes this mapping in a compact dictionary.

This dictionary allows one to use the compact RF language (phase rotators, RF Cells, $\alpha(d)$) while retaining a clear route back to standard microscopic theory.

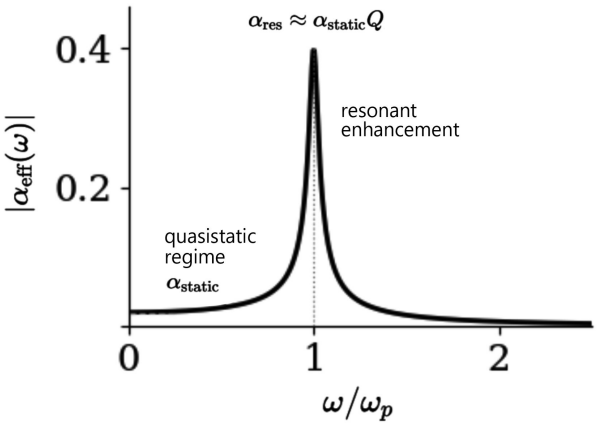

Fig.6 Bridge

Figure 5: Schematic frequency dependence of $|\alpha_{\text{eff}}(\omega)|$: a small static value in the quasistatic regime and a resonant enhancement near $\omega = \omega_p$ by a factor of order Q.

5 Conclusion

We have constructed a bridge between the conceptual Resonant Field view of superconducting weak links and the standard microscopic description based on GL/Usadel equations, London–Maxwell electrodynamics, and the RCSJ model.

- In Part I we formulated the RF framework: weak links as phase rotators, the notion of a Resonant Field Cell, the Phase–Control Equation, and the key parameter α that measures how efficiently a local microcoil can rotate the Josephson phase.
- In Part II we showed how the same phenomena arise from classical theory: the dependence of $I_c(d)$ and phase profiles on thickness, the role of localized modes in thick SNS bridges, and the oscillator estimate $\alpha_{\text{res}} \approx \alpha_{\text{static}} Q$ for resonant enhancement of the phase response.
- In Part III we provided an explicit mapping between RF concepts and classical objects, allowing the RF framework to be used as a compact high-level language while remaining grounded in established physics.

Conceptually, the framework developed here extends the conventional view in which a strong magnetic influence on the Josephson phase is typically associated with a macroscopic loop (SQUID geometry). Once localized modes in thick SNS weak links are taken into account, a single weak link can in principle reach phase–flux couplings in the range $|\alpha| \sim 0.3$–0.6 under resonant driving by a local microcoil.

Potential applications of the strong-rotator regime include: (i) local magnetic control of Josephson qubits and oscillators without global bias fields, (ii) ultra-compact SQUID-like magnetometers where the effective phase–flux coupling is provided by a single thick weak link, and (iii) coil-driven Josephson oscillators and parametric devices where RF excitation is applied locally via microcoils rather than global microwave lines. The parameter α provides a natural figure of merit for the design of such devices.

A Oscillator derivation of the relation $\alpha_{\text{res}} \approx \alpha_{\text{static}} Q$

In this appendix we collect the standard oscillator derivation of the relation $\alpha_{\text{res}} \approx \alpha_{\text{static}} Q$ used in the main text.

Resonant Field framework		Classical description
Phase field $\phi(\mathbf{r})$	$\longleftrightarrow$	Order-parameter phase $\theta(\mathbf{r})$ (GL/Usadel)
Phase rotator	$\longleftrightarrow$	Weak link with large $\partial\varphi_J/\partial\Phi_{\text{ext}}$
Resonant Field Cell	$\longleftrightarrow$	Localized GL+Maxwell mode (phase, j_s, B) near the weak link
Phase–flux coefficient α	$\longleftrightarrow$	$\alpha(d,\omega) = \frac{\Phi_0}{2\pi}\left.\frac{\partial\varphi_J}{\partial\Phi_{\text{ext}}}\right\|_\omega$
Phase–Control Equation	$\longleftrightarrow$	Linearized RCSJ with external flux (small-signal phase–flux relation)
Strong–rotator regime	$\longleftrightarrow$	Thick SNS, $d \sim \xi$, with $\alpha_{\text{res}} \simeq \alpha_{\text{static}} Q \sim 0.3$–$0.6$

Figure 6: Mapping between the Resonant Field framework and the classical description. Each RF object (phase field, phase rotator, Resonant Field Cell, α, the Phase–Control Equation, and the strong-rotator regime) has a direct counterpart in the standard GL/Usadel + London–Maxwell + RCSJ formulation.

Linearizing the RCSJ equation around a static operating point and including a small coil current $I_{\text{coil}}(t)$, we obtain

$$C\ddot{\varphi} + \frac{1}{R}\dot{\varphi} + \frac{1}{L_J}\,\varphi = K I_{\text{coil}}(t), \tag{A.1}$$

which is a driven damped harmonic oscillator with natural frequency

$$\omega_p = \sqrt{\frac{1}{L_J C}} \tag{A.2}$$

and damping rate

$$\gamma = \frac{1}{2RC}, \tag{A.3}$$

so that the quality factor is

$$Q = \frac{\omega_p}{2\gamma} = \omega_p RC. \tag{A.4}$$

For a harmonic drive

$$I_{\text{coil}}(t) = I_0 \cos\omega t, \tag{A.5}$$

the steady-state response can be written as

$$\varphi(t) = \Re\{\tilde{\varphi}(\omega) e^{i\omega t}\}, \qquad \tilde{\varphi}(\omega) = \frac{K I_0}{-C(\omega^2 - \omega_p^2) + i(2\gamma C\omega)}. \tag{A.6}$$

The amplitude is therefore

$$|\tilde{\varphi}(\omega)| = \frac{|K| I_0}{\sqrt{(\omega_p^2 - \omega^2)^2 + (2\gamma\omega)^2}}. \tag{A.7}$$

Identifying $\Phi_{\text{ext}} = M I_{\text{coil}}$ and using the definition of $\alpha_{\text{eff}}(\omega)$ via

$$\delta\varphi(\omega) = \alpha_{\text{eff}}(\omega)\,\frac{2\pi}{\Phi_0}\,\Phi_{\text{ext}}(\omega) = \alpha_{\text{eff}}(\omega)\,\frac{2\pi}{\Phi_0}\,M I_0, \tag{A.8}$$

we obtain

$$\alpha_{\rm eff}(\omega) = \frac{|\delta\varphi(\omega)|}{(2\pi/\Phi_0)MI_0} = \frac{|K|\Phi_0}{2\pi M}\frac{1}{\sqrt{(\omega_p^2-\omega^2)^2+(2\gamma\omega)^2}}. \tag{A.9}$$

In the quasistatic limit $\omega \ll \omega_p$ we have

$$\alpha_{\rm static} \equiv \alpha_{\rm eff}(0) \approx \frac{|K|\Phi_0}{2\pi M}\,\frac{1}{\omega_p^2}, \tag{A.10}$$

while at resonance ($\omega = \omega_p$),

$$\alpha_{\rm res} \equiv \alpha_{\rm eff}(\omega_p) = \frac{|K|\Phi_0}{2\pi M}\,\frac{1}{2\gamma\omega_p}. \tag{A.11}$$

Eliminating the prefactor via $\alpha_{\rm static}$ yields

$$\alpha_{\rm res} \approx \alpha_{\rm static}\,\frac{\omega_p}{2\gamma} = \alpha_{\rm static}Q, \tag{A.12}$$

which is the relation used in Sec. 3.7 and in the RF framework discussion.

B Order-of-magnitude estimate for a thick SNS bridge with microcoil

The oscillator relation $\alpha_{\rm res} \approx \alpha_{\rm static}Q$ shows that a modest static coupling $\alpha_{\rm static}$ can be amplified into a strong-rotator regime at resonance, provided the mode has a reasonable quality factor Q. Here we collect a simple numerical estimate for a thick SNS bridge addressed by an on-chip microcoil.

Consider a diffusive SNS weak link with

- normal-layer thickness $d \sim 10$ nm,
- width $w \sim 300$ nm,
- coherence length ξ such that $d \sim \xi$ (thick SNS regime),
- London penetration depth in the electrodes $\lambda_L \sim 250$ nm.

For such dimensions the effective kinetic inductance of the weak-link region can be of order

$$L_{\rm kin} \sim 20\text{–}30 \text{ pH}, \tag{B.1}$$

while realistic planar microcoils placed above the bridge can reach mutual inductances in the range

$$M \sim 0.8\text{–}1.8 \text{ pH}. \tag{B.2}$$

In a simple lumped picture the static phase–flux coupling can be estimated as

$$\alpha_{\rm static} \sim \frac{M}{L_{\rm kin}} \sim 0.03\text{–}0.07, \tag{B.3}$$

which already lies two–three orders of magnitude above the tunnel-junction values $|\alpha_{\rm static}| \sim 10^{-3}$–$10^{-2}$ quoted in the main text for typical SIS geometries.

For localized plasma-like modes in the 5–20 GHz range, quality factors of order

$$Q \sim 15\text{–}35 \tag{B.4}$$

are not unreasonable for carefully engineered on-chip structures. Combining the two estimates, we obtain a resonant phase–flux coupling

$$|\alpha_{\mathrm{res}}| \sim |\alpha_{\mathrm{static}}|\, Q \sim 0.3\text{–}0.6, \tag{B.5}$$

which falls squarely into the target strong-rotator window of the RF framework.

This back-of-the-envelope estimate does not replace full GL/Usadel + London–Maxwell simulations, but it shows that thick SNS bridges with realistic microcoils can, in principle, reach the strong-rotator regime without requiring extreme values of M, L_{kin}, or Q. It also motivates the experimental programme described in Ref. [4], where coil-driven Shapiro steps in such devices are proposed as a direct operational probe of $\alpha(d, \omega)$.

Acknowledgements

The author thanks colleagues and collaborators for discussions on SNS weak links, localized modes and resonant control of Josephson phase.

References

[1] A. Turchanov, *Resonant Field Symmetry in Superconductors: A Standing-Wave Picture of Meissner Screening and Josephson Barriers*, Phase Geometry Series — Part I, preprint (2025).

[2] A. Turchanov, *Phase-Coherent Josephson Devices as Clocks in Weak Gravitational Fields*, Phase Geometry Series — Part II, preprint (2025).

[3] A. Turchanov, *Phase-Field Newtonian Gravity and Phase Clocks*, Phase Geometry Series — Part III, Zenodo (2025).

[4] A. Turchanov, *Magnetic Phase Control of a Thick SNS Weak Link*, experimental proposal / preprint (2025).